Hindawi
International Journal of Antennas and Propagation
Volume 2022, Article ID 4809313, 10 pages
https://doi.org/10.1155/2022/4809313

*Research Article*

# Using the WSPR Mode for Antenna Performance Evaluation and Propagation Assessment on the 160-m Band

**Jurgen Vanhamel**,[1,2,3] **Walter Machiels**,[4] **and Hervé Lamy**[5]

[1]*TU Delft Faculty of Aerospace Engineering, Section Space Systems Engineering, 2629 HS Delft, Netherlands*
[2]*KU Leuven, Electronic Circuits and Systems, Geel 2440, Belgium*
[3]*Royal Belgian Institute for Space Aeronomy, Engineering Division, Brussels 1180, Belgium*
[4]*Amateur Radio Observer, Member of the Royal Belgian Amateur Radio Union (UBA), Sint-Truiden 3800, Belgium*
[5]*Royal Belgian Institute for Space Aeronomy, Division of Space Physics, Brussels 1180, Belgium*

Correspondence should be addressed to Jurgen Vanhamel; j.a.m.vanhamel@tudelft.nl

Received 31 January 2022; Revised 14 June 2022; Accepted 21 June 2022; Published 15 July 2022

Academic Editor: Shobhit K. Patel



In the last couple of years, the use of weak signal propagation reporter (WSPR) has grown significantly in the radio amateur community and beyond. This protocol allows to probe potential propagation paths between radio transceivers, operating at a low-power level. The protocol decodes the received signals and translates them into appropriate signal-to-noise ratio levels, which reveal the possible propagation paths between the transmitter and receiver using ionospheric reflections. In this article, specifically the 160-m radio amateur band is addressed. This band used less intensity for WSPR communication, compared to the other radio amateur bands (80 m and 40 m). Additionally, the 160-m band has specific features such as the link between propagation performance and the Earth's electron gyro-effect. The aim of this article is to address these features experimentally. First, two identical 160-m band WSPR receiver stations are conditioned to compare the performance of different 160-m band antennas. Each setup, separated by a limited distance, generates almost identical SNR reports, allowing the comparison between the two antennas. Second, a more extended experimental investigation of the propagation path performance on the 160-m band reveals information on the radio wave behaviour between the transmitter and receiver. The first experiment allowed the identification of the most optimal antenna, specifically in the 160-m band. The second experiment shows that the SNR values can vary depending on the polarization shift of the received signal. Possibly, this can be linked to the effect of the magnetic field of the Earth via the electron gyro-frequency.

## 1. Introduction

The use of shortwave communication (below 30 MHz), using reflection against the ionosphere, is common in a wide variety of applications, that is, emergency, maritime, aeronautical, press, ionospheric sounding, and radio amateur communications. The main advantage of using ionospheric reflection is the ability to communicate beyond the line of sight. The accompanying disadvantage is the variability of the behaviour of the different ionospheric reflection layers. Physical changes in the ionosphere, such as day-night dichotomy, solar activity, and the intensity of the magnetic field of the Earth, all have an effect on the certainty of the radio connection between the transmitter and the receiver. Additionally, the used setup and performance of the receiving system also have an effect. Hence, a good knowledge of the performance of the used antenna and of the ionospheric behaviour is mandatory in order to evaluate the connection.

In the frame of shortwave communication, radio amateurs often use digital modulation techniques to transmit and receive information. Weak signal propagation reporter (WSPR) is one of the many digital modes available for communication purposes used by radio amateurs around the world. The protocol uses a narrow reference bandwidth of only 2500 Hz in the LF, MF, and HF bands for radio

amateurs. Other modes for digital communication are, for example, FT8, FT4, JT4, JT9, JT65, and QRA64 [1].

WSPR has been used to analyse the behaviour of antennas [2–5], or to investigate the behaviour of the ionosphere and to analyse propagation prediction [6, 7]. For example, the High-Frequency Active Auroral Research Program (HAARP) used WSPR to model the ionosphere [8] and to study the propagation effects in the frequency range of 3 Hz to 30 kHz by using different uplink angles with respect to the magnetic field lines of the Earth [9]. The same facility was used in the 40-m (7.0 to 7.2 MHz) and 80-m (3.5 to 3.8 MHz) radio amateur band for propagation research [10]. Even in the very-high-frequency (VHF) band, WSPR was used for propagation analysis [11]. Also recently, the WSPR mode was used for evaluating radio propagation in the Southern Hemisphere [12].

WSPR should be seen as a propagation prediction mode, rather than a bi-directional communication principle. The goal is to use low-power transmitters and investigate which distance can be bridged using ionospheric reflections in the shortwave range. Transmitted radio waves reaching the ionosphere are bended back to Earth based on progressive refraction. Throughout this path, the radio waves experience multiple effects, such as absorption, and temporal and spatial ionospheric disturbances, each influencing the range of the transmission [13]. Using the secant law, the single reflected bridged distance $d$ can be calculated in a simplified manner [14]:

$$d = 2.H\sqrt{\sec^2(\theta_i) - 1}, \quad (1)$$

where $H$ is the height above the ground of the mirror and $\theta_i$ is the incident angle of the radio wave related to the vertical. To calculate this bridged distance, WSPR uses a dedicated database system [15] in which all successful propagation paths are listed together with their signal-to-noise ratio (SNR) value. By uploading these reception reports into the central database, an extended overview of different propagation paths is created. Hence, an outline can be made for all possible communication paths for a specific transmitter station.

The purpose of this study is twofold. First, showing that the existing WSPR transmitter infrastructure can be used to investigate the performance of two distinct antenna systems situated at (nearly) the same location, specifically in the 160-m radio amateur band (1.8 up to 2 MHz). Also the low-frequency range of this band falls within the Earth's electron gyro-frequency range (from roughly 0.7 MHz up to 1.6 MHz [16, 17]). This can maybe be linked to the reflection effectiveness of radio waves and to the behaviour of the ionosphere. By comparing an extensive dataset of measurements, using two identical receiver setups, a performance characterization overview of the two antennas can be created. Second, by using an antenna setup sensitive to polarization, the obtained dataset may reveal information on the electromagnetic wave propagation behaviour in the 160-m band. Indeed, when a radio wave is reflected by the ionosphere, two modes of propagation (ordinary and extraordinary) are formed due to the birefringent effect.

Similar studies on radio wave propagation analysis in the ionosphere and antenna performance evaluation have been carried out using a Near-Vertical-Incidence-Skywave (NVIS) antenna setup [18–21]. These studies were applied at several shortwave frequencies but not the 160-m band. Moreover, they used a dedicated more complex transmitter-receiver link than the setup proposed in this article. The advantage of this research is that it makes use of an already existing transmitter infrastructure, that is, the radio amateur WSPR stations. Currently, one disadvantage is that the polarization state of the transmitted signals is unknown.

The novelty of this study lies in (1) the use of the existing WSPR transmitter infrastructure as an evaluation tool for NVIS antenna performance analysis, specifically in the 160-m band and (2) the use of the same WSPR mode for ionospheric propagation analysis in the 160-m band. Based on the recent review study of Hervás et al. [22], the use of WSPR as an assessment tool for ionospheric propagation is novel.

## 2. The WSPR Protocol

Originally, the protocol was named Manned Experimental Propagation Tests, by Joe Taylor (MEPT_JT) [23]. Later, the acronym was changed to WSPR. The protocol works in a narrow reference bandwidth of 2500 Hz, in which only 50 bits are transmitted, occupying only 6 Hz bandwidth for each transmission. The WSPR protocol uses the same convolution code for his forward error correction (FEC) as the JT4 mode. Hence, the constraint length $K = 32$ at a rate of $r = 0.5$ results in 162 binary channel symbols at a baud rate of 1.46 baud [23]. By using this long constraint length, undetected errors are less common. The drawback is the use of a less efficient and simpler sequential algorithm instead of the more enhanced Viterbi algorithm [23, 24].

The message itself contains three parts: (1) the call sign of the transmitting radio amateur station, (2) the 4-digit locator of the transmitting station, and (3) the power level of the transmitter in dBm. The call sign occupies 28 bits, the grid locator 15, and the power level 7, which makes in total 50 bits. Each transmission occupies 110.6 seconds and starts one second into an even Universal Time Coordinated (UTC) minute [25]. The total time the WSPR software "listens" is two minutes, after which the software decodes the signals and displays the received stations, the SNR levels, and the distances between transmitter and receivers. The minimal received detectable SNR value is −34 dB, using 2500 Hz bandwidth as a reference.

WSPR uses frequency shift keying (FSK) as a modulation method to transfer the information. The sent message contains the call sign of the radio amateur, the grid locator parameter, and the level of power used by the transmitting station (in dBm). All this information is suppressed into a 50-bit wide message. The station setup consists of a computer running applicable software (i.e., WSJT [26]), which is able to decode and generate the WSPR message.

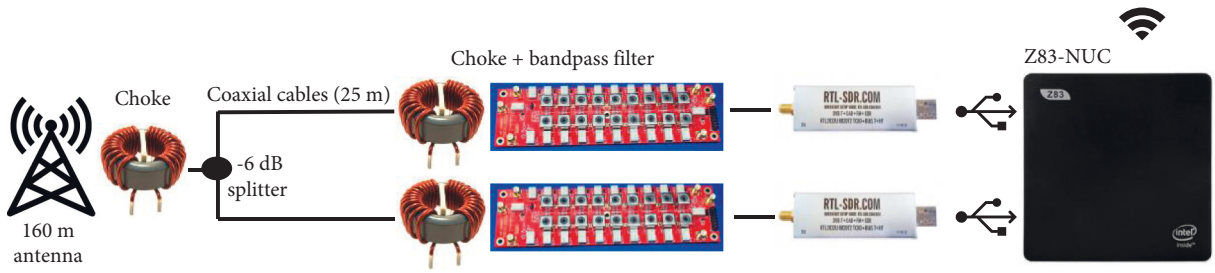


Figure 1: Double identical WSPR receiver setup using two RTL dongles, the ITA LWA II long wire antenna, and a power splitter for calibration purposes.

## 3. Method of Analysis

In this section, the infrastructure, all peripherals, and the used test method are described. The setup of this study consists of two identical receiver stations, each composed of an RTL dongle Software Defined Radio (SDR), filters at the antenna and receiver sides, a battery powered Z83-NUC mini PC, WSJT software [26], and 160-m antennas. The RTLs are both connected to the same Z83-NUC in order to avoid discrepancies in the processing of the signals received. The Z83-NUC runs on batteries and is connected to the Internet via Wi-Fi in order to avoid any common mode or interference of unwanted signals. The RTL dongles are directly plugged into the Z83-NUC, without using any additional cables. The coaxial and other cables for the two stations are similar and have the same length. Hence, a double, identical receiver station is created.

First, for calibration reasons, the two RTL dongles are connected to the same antenna in order to compare the performance of both receivers (Figure 1). The used antenna is an ITA LWA II 20-meter-long wire antenna [27], containing a balun-choke combination at the input and connected using a splitter network of −6 dB. The latter is a passive three-resistor network, in which each resistor is 16.7 Ohm. On each receiver line, an additional choke is used, combined with a band-pass filter [28]. These filters allow to only select the applicable band in which measurements are taken (160-m band). The used filter is a selectable filter, containing 10 separate pass-bands. Relays are used to activate one band-pass filter at a time, as selected by the control connector pins. The relays are powered from a 5 V DC input, while the selection is done by applying a 3.3 V (or 5 V DC)—TTL "HIGH" to each metal-oxide-semiconductor field-effect transistor's (MOSFET) gate. Each band-pass filter uses two variable shielded inductors and three capacitors. An attenuation of 7 dB is attained due to the use of these passive filters. Both band-pass filters are calibrated using a VNA (vector network analyser) in order to assure the same band-pass behaviour in both receiver chains.

The common-mode chokes are made of 16-mm clamp-on mix31 ferrite and two twisted CAT5-pairs (Zo = 100 Ohm) in parallel, but wound in the opposite direction. Hence, an overall impedance of 50 Ohm is retained while creating a high choke impedance. These devices avoid picking up high-frequency signals and allow the setup to measure the performance of the antennas without the transmission lines contributing to the reception of signals. In detail, these chokes are 1 : 1 baluns, isolating the outer surface of the shield of the coax from the feed point terminals. They also lower the re-radiation from common-mode current that distorts the antenna pattern. Additionally, they prevent high-frequency noise picked-up by the coax shield from entering the feedline [29]. The length of the coaxial cables is 25 m each. The chokes and band-pass filters are mounted inside a dedicated mechanical enclosure (Figure 2). The performance of both receiver chains is investigated by comparing the SNR of real received signals. At both receivers, the deviation performance factor of each RTL dongle is found, which is additionally used to level out any performance difference between the two receiver chains.

After averaging out this variance, in the first experiment, a specific (but different) 160-m antenna is connected to each RTL dongle, using the setup described in Figure 3. The first 160-m antenna is a homebrew adapted shorted dipole [30]. The used antenna is adapted compared to the original shorted dipole design: (1) the orientation is horizontal instead of vertical to increase near vertical radiation behaviour, (2) the length-diameter ratio of the stainless steel dipoles is raised in order to increase the bandwidth of the antenna, (3) a common-mode choke is implemented on the coil to lower transmission line radiation, and (4) the coil is mounted under 45° to lower the influence of metal on the performance of the antenna.

The second 160-m antenna is the commercial ITA LWA II 20-meter-long wire antenna [27]. Both antennas are mounted on top of a mast at a height of 15 m (Figure 4).

In the first experiment, the double receiver station allows to investigate the performance of two different 160-m antennas at different orientations, in order to characterize the performance of the antennas.

Additionally, as a second experiment, the measurement of the effect of polarization change to which an electromagnetic wave is subject during the reflection against the ionosphere is aimed at. First two different and then two identical 160-m band antennas are used in the setup described in Figure 3. Both antennas are physically shifted by 90° in the horizontal plane of the Earth. Hence, the effect of polarization should be detectable. Consequently, conclusions may be drawn on the propagation behaviour of the received radio waves.

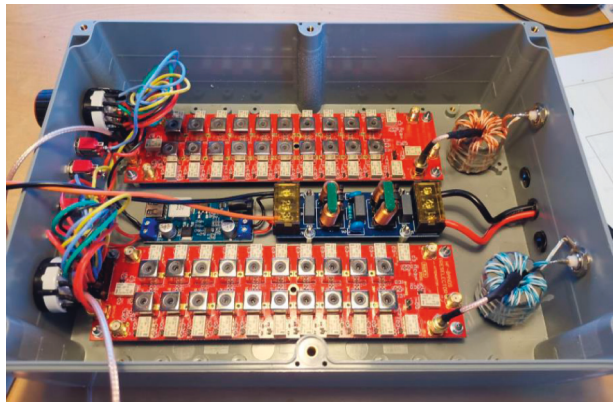

Figure 2: The assembled chokes and band-pass filters for both receiver chains.

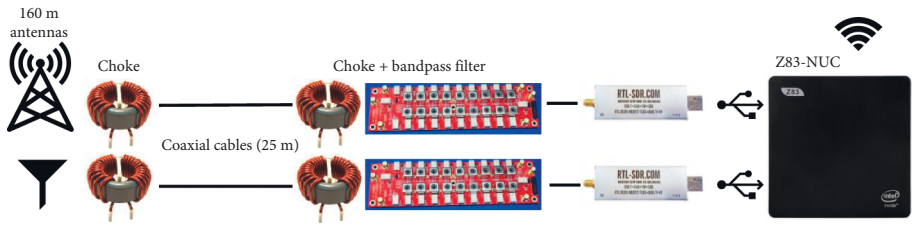


Figure 3: Double identical WSPR receiver setup using two RTL dongles connected to two different 160-m antennas (adapted shorted dipole and the ITA LWA II).

Figure 4: The adapted shorted dipole and the ITA LWA II 20-meter-long wire antenna (from top to lower right).

## 4. Results and Discussion

The performance of the two receiver chains was first investigated in order to calibrate the double receiver setup. Both receiver chains are connected to a single 160-m antenna as illustrated in Figure 1. The RTL dongles did not use any hardware or audio AGC (automatic gain control). The same settings were applied in the WSJT software for both receiver chains. This setup ran for seven consecutive days in order to have a valid dataset to do the calibration of both receiver chains. Only those stations who were received more than 50 times during these seven days were taken into account. Based on this dataset, an average difference of 1.2 dB was noted between the two receiver chains. Later on, another period of seven days measurements was performed to confirm this result. The same average deviation of 1.2 dB was

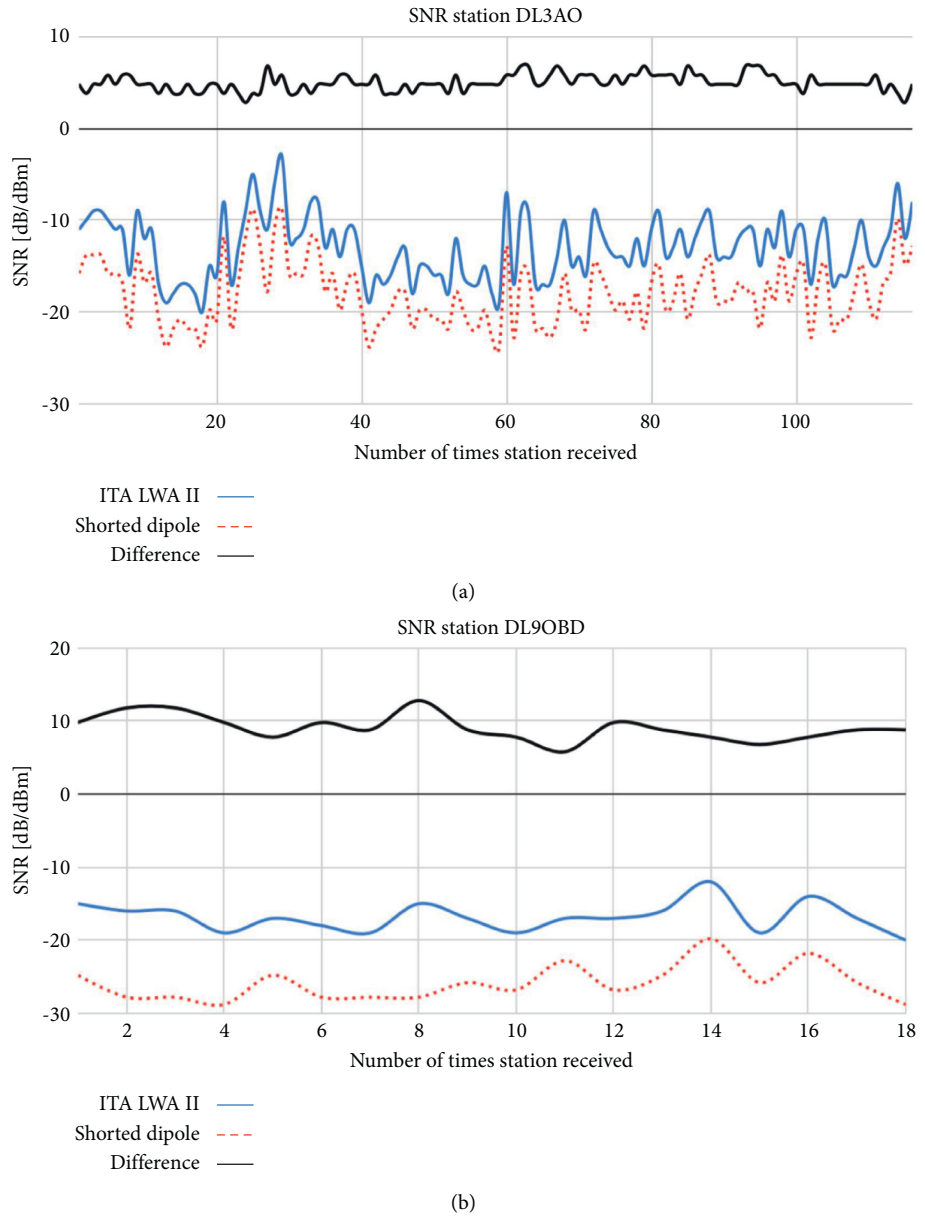


FIGURE 5: The SNR values of both 160-m antennas for two received stations. The solid blue line is the ITA LWA II antenna, and the dotted red line is the adapted shorted dipole. The difference between both SNR values is shown at the top of both charts as a solid black line. (a) Received SNR values of station DL3AO. (b) Received SNR values of station DL9OBD.

measured between the two receiver chains and will be taken into account in the result comparison in the next paragraphs.

*4.1. Antenna Performance Comparison.* Now that two reliable and calibrated receiver chains are build, the setup described in Figure 3 is used to compare the performance of two different 160-m antennas. The two antenna configurations are located in the authors' backyard, almost at the same position (Figure 4). Consequently, nearly the same signals are captured by both antennas.

The measurements were performed over a time period of seven days. Hence, a dataset was obtained, covering hundreds of received signals from different locations, spread 360° around the antennas. In a process to avoid all outliers with excessive values, only those stations which are received >10 times by both receiver chains are taken into account.

The SNR values received by both receiver chains for two random stations are shown in Figures 5(a) and 5(b). The solid blue line illustrates the reception performance of the ITA LWA II antenna, while the dotted red line shows the performance of the adapted shorted dipole. The difference between both graphs is shown at the top of each figure as a solid black line. On the horizontal axis, the number of times the station is received is shown. The 1.2 dB correction factor is applied to all the SNR values. The graphs clearly show the performance difference between the two used 160-m antennas.

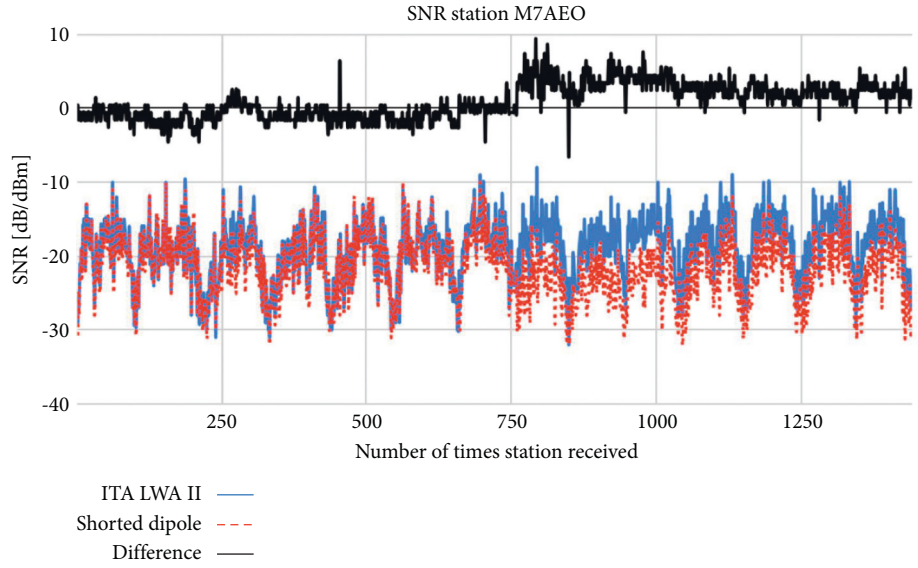


Figure 6: The SNR values of antennas for station M7AEO. The solid blue line is the ITA LWA II antenna (two weeks in the same position), and the dotted red line is the adapted shorted dipole (one week in parallel with the ITA LWA II antenna—up to measurement point 750, in the second week shifted by 90° in the horizontal plane—after measurement point 750). The difference between both SNR values is shown as a solid black line at the top of the chart.

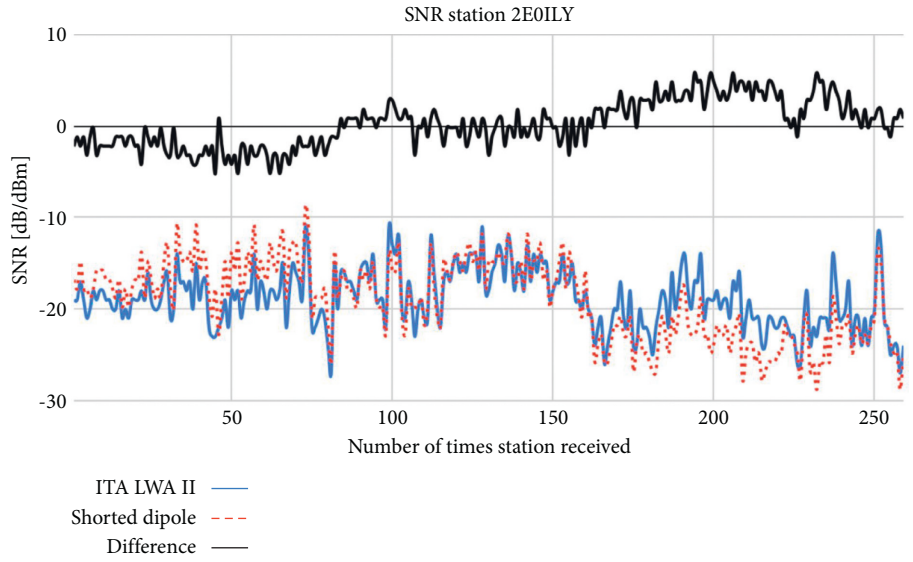


Figure 7: The SNR values of both 160-m antennas for the received station 2E0ILY. Between measurement points 0 and 110, both antennas are in parallel. Between measurement points 110 and 255, the adapted shorted dipole antenna is shifted by 90° in the horizontal plane, compared to the ITA LWA II antenna. The solid blue line is the ITA LWA II antenna, and the dotted red line is the adapted shorted dipole. The difference between both SNR values is shown at the top of the chart (solid black line).

In Figure 5(a), the received SNR values of station DL3AO are shown. A difference of around 5 dB (minimum value = 3 dB, maximum value = 7 dB) is noticed between the two antennas (solid black line at the top of the chart).

In Figure 5(b), the received SNR values of station DL9OBD are shown. At certain measurement points, a performance difference can be observed between both antennas. At measurement point 5, the dotted red line shows a peak, while the solid blue line does not. At measurement point 8, the situation is reversed. Hence, the difference between both antennas varies from 6 dB up to 13 dB (solid black line at the top of the chart in Figure 5(b)). This indicates a performance difference between both antennas.

It has to be noted that the directivity of both antennas is not investigated in the previous experiment. To characterize the directivity of the antennas using WSPR, the two antennas (adapted shorted dipole and the ITA LWA II antenna) were placed one week in a parallel horizontal plane, and the next week the adapted shorted dipole was shifted by 90° in the same horizontal plane, in relation to the ITA LWA

Figure 8: The two identical adapted shorted dipoles shifted by 90° in the horizontal plane.

II antenna. In Figure 6, the results are shown for the M7AEO station. A clear difference can be seen after one week (at measurement point 750 in Figure 6). A "step-up" (solid black line in the top of Figure 6) in performance difference is noticed when the adapted shorted dipole is shifted by 90°. This behaviour is similarly seen for all received stations, spread randomly around the receiver antennas, so not only for those related to a specific direction (i.e., north-south or east-west). The measured difference between week 1 and week 2 varies for all stations in a range from 1 to 3 dB. Also, for this particular station for which many points are available, the effect of day and night is clearly observable in Figure 6 with a wide variation in signal strength of up to 22 dB.

A possible explanation of this "step-up" can be found in the characteristics of the antenna, but may also be linked to the reflection effectiveness and behaviour of the different layers in the ionosphere (D-layer, E-layer, and so on). The magnetic field also modifies the polarization of both ordinary and extraordinary waves and the index of refraction [31]. This is investigated in the next section.

*4.2. Propagation Assessment: Part 1.* The refraction index of the ionosphere depends on the magnetic field of the Earth via the gyro-frequency of the electrons in the E region and on collisions at lower altitudes (D region). This is the well-known Appleton equation (see, e.g., equation 3.8 in Davies [32]). For the propagation of the radio wave at an oblique angle with respect to the magnetic field of the Earth, two modes of propagation exist: the ordinary and extraordinary waves, each with different polarizations. As described by Maso et al. [33], the polarization of received signals can change due to the refraction of the electromagnetic wave in the ionospheric layers with ordinary and extraordinary reflected rays having distinct properties like a slight shift in frequency, amplitude, phase, and arrival time at the receiver antenna. Witvliet et al. [18] showed that a signal difference of 13 dB can occur between the ordinary and extraordinary waves, using a high-power setup transmitter (800 W) at a frequency of 5.39 MHz.

To investigate this effect, we present in Figure 7 another set of measurements, obtained using the setup of Figure 3 and the approach discussed in paragraph 4.1. Again, an odd behaviour of the received signals on both antennas is noticed. On the left and right sides of the graph, a "swap" is noticed between the SNR values of both antennas. The performance of the adapted shorted dipole (dotted red line) shows a better reception of station 2E0ILY from measurement point 0 up to 110, while after measurement point 110 (the adapted shorted dipole is now shifted by 90°), the situation is reversed. This phenomenon may be due to different propagation characteristics of the received signals, with a possible change in the polarity of the signal received by both antennas. Indeed, the sensitivity of both antennas to polarization of the incoming signal might be different, which would lead to the observed change in SNR.

*4.3. Propagation Assessment: Part 2.* As an attempt to distinguish between the atmospheric effects and the performance difference of both antennas, an additional experiment, using WSPR in the 160-m band, was necessary. This was done by placing two identical adapted shorted dipoles (instead of two different types) at an angle of 90 degrees in the horizontal plane (see Figure 8) using the setup described in Figure 3. Both antennas were tuned to the same frequency. Hence, the two receiver chains were able to compare the effect of polarization using the received SNR values. The only difference between the two receiver chains was the orientation of the antenna.

During a measuring period of two weeks and receiving random stations spread 360° around the antennas, again the dataset only contains those stations that are received >10 times by both receiver chains. As an example, the received SNR values for station 2E0ILY and M7AEO for both receiver chains are shown in Figures 9(a) and 9(b). Comparing the graph of the 2E0ILY station in Figure 7 with Figure 9(a) shows again the effect of signal increase if the antenna is shifted by 90°. The same conclusion is valid for the SNR values of station M7AEO. Comparing Figure 9(b) with

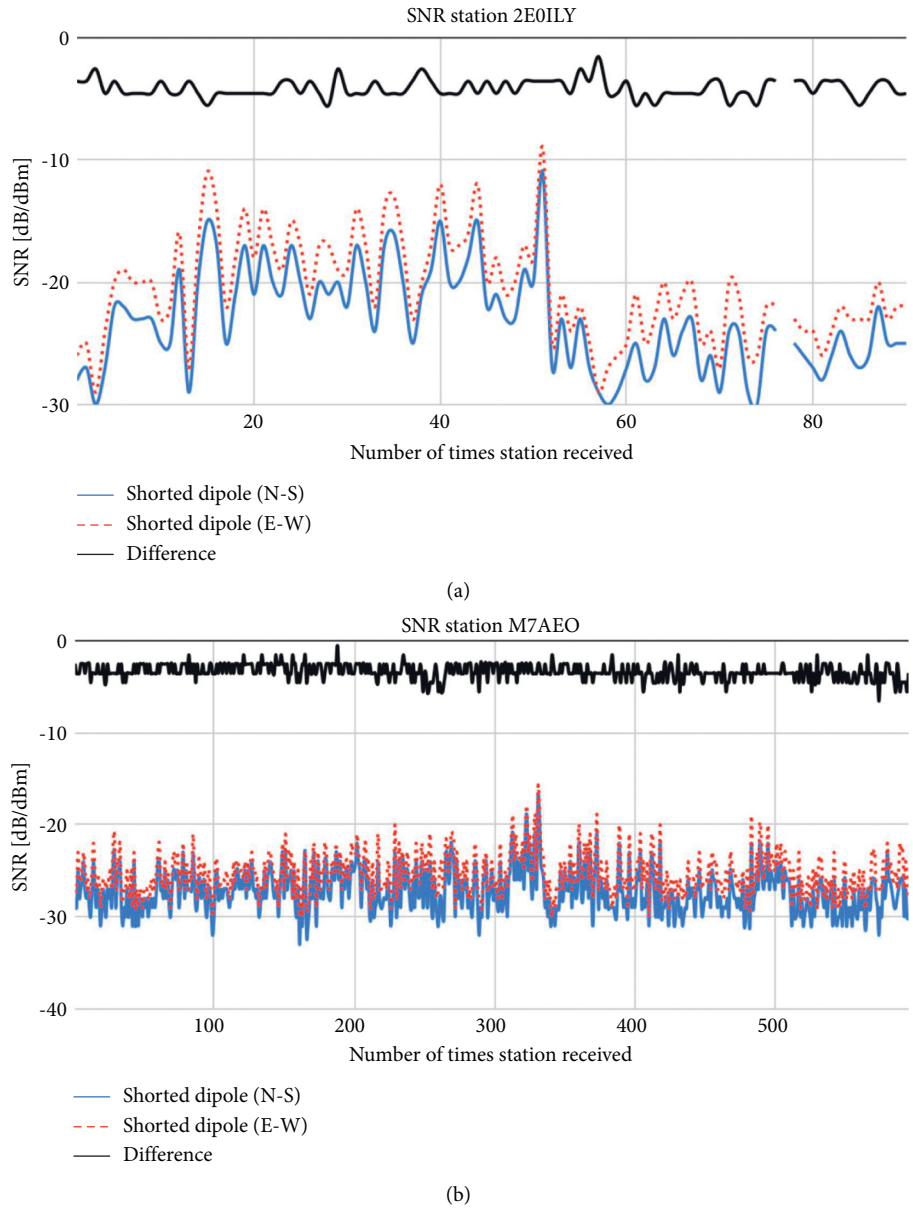


Figure 9: The SNR values of both adapted shorted dipoles for reception of the 2E0ILY and M7AEO stations (a and b). In each figure, the solid blue line represents the first adapted shorted dipole positioned in the north-south direction, and the dotted red line the second adapted shorted dipole positioned in the east-west direction. The difference between both SNR values is shown at the top of both charts as a solid black line. (a) Received SNR values for both antennas of station 2E0ILY. (b) Received SNR values for both antennas of station M7AEO.

Table 1: Summary of the SNR differences obtained during the comparisons between antennas carried out during this study.

| Station | Adapted shorted dipole vs. ITA LWA II antenna | | Two identical adapted shorted dipoles |
|---|---|---|---|
| | Antennas not shifted (dB) | Antennas shifted by 90° (dB) | Antennas shifted by 90° (dB) |
| M7AEO | −4 to +2 | +1 to +6 | −5 to −2 |
| 2E0ILY | −5 to +2 | −3 to +5 | −5 to −2 |
| Average SNR difference (when shifted by 90°) (dB) | | 3 | 3 |

Figure 6 clearly shows the effect of turning the antenna by 90°. In Figures 9(a) and 9(b), the comparison between the two positions reveals an advantage of using the adapted shorted dipole in the east-west direction by around 3 dB. This conclusion is also valid for other measured stations and is not limited to one specific geographical location of a

received station. For all randomly spread received stations, an increase of around 3 dB was noticeable. A possible hypothesis is the reflection effectiveness and characteristics of the different ionospheric layers. Again, the electron gyro-effect and the intensity of the magnetic field of the Earth can play a significant role as discussed in paragraph 4.1 [16, 17, 31].

## 5. Conclusions

The discussed method consists in (1) setting up a calibrated double receiver chain, in order to analyse the performance of two antennas and (2) investigating the propagation effects on the received radio waves. These experiments were carried out using the WSPR mode, specifically in the 160-m radio amateur band.

Comparing the received signals over a sufficiently long time period, using one antenna and two receivers, has allowed the authors to accurately calibrate the two receiver chains. Additionally, the performance of two antennas can be characterized up to a certain level. Indeed, the received SNR values can vary (1) on the performance difference and directivity of the antennas and (2) on the polarization shift of the received signals as illustrated in the second experiment. The latter effect is due to ionospheric effects. In order to investigate this in more detail and being able to disentangle between the two effects, a better knowledge of the polarization of the transmitted signals is required and could possibly be considered in the future.

From a practical point of view, the results clearly show that an SNR improvement is possible by orienting the antenna in a specific direction, independent of the used antenna system. To illustrate this, the authors compared the SNR difference caused by the effect of 90° shifting of an adapted shorted dipole and an ITA LWA II antenna on the one hand and two identical adapted shorted dipoles on the other hand. In Table 1, a summary of the comparisons of the setups is provided in a tabular form.

For both configurations, the same SNR difference of around 3 dB is seen if a 90° shift is imposed between the two antennas. It therefore seems to indicate a link with the ionospheric effects although this needs further investigation.

Additional further research could consist in evaluating other orientations between the two identical adapted shorted dipoles (e.g., shift by 30°, 45°, and 60°) and measure the effect on the received SNR. The same can be done to investigate the directivity of the antennas. Hence, a detailed antenna radiation diagram can be obtained. These experiments can be the subject of a follow-up research.

## Data Availability

The data used to support the findings of this study are available from the corresponding author upon request.

## Conflicts of Interest

The authors declare that there are no conflicts of interest regarding the publication of this article.

## Acknowledgments

This work was supported by the Royal Belgian Institute for Space Aeronomy, the Royal Belgian Amateur Radio Union, and the Radio Amateur Community.

## References

[1] H. W. Silver, "Structures digital modes," in *The ARRL Handbook for Radio Communications 2021*, E. McCune, Newington, CT, USA, 98 edition, 2020.

[2] G. Griffiths and R. Robinett, *Aids to the presentation and analysis of wspr spots: timescaledb database and grafana*, in *Proceedings of the 2020 ARRL TAPR Digital Communications Conference*, Charlotte, CA, USA, September 2020.

[3] G. Griffiths and N. Squibb, "Improving HF Band SNR from analysis of WSPR spots," *Practical Wireless*, vol. 93, pp. 23–26, 2017.

[4] WSPR, "Evaluation of two160m RX-antennas using WSPR reports," 2021, https://f6irf.blogspot.com/2008/04/wspr-evaluation-of-two160m-rx-antennas.html.

[5] C. F. Milazzo, "Comparative antenna analysis with WSPR. using the weak signal propagation reporter network to compare antenna performance," 2021, https://www.qsl.net/kp4md/wspr.htm.

[6] B. A. Witvliet, E. van Maanen, G. J. Petersen et al., "Measuring the isolation of the circularly polarized characteristic waves in nvis propagation, " [measurements corner]," *IEEE Antennas and Propagation Magazine*, vol. 57, no. 3, pp. 120–145, 2015.

[7] T. Dutono, Z. Zakariyah, T. Santoso, and D. Setiawan, "A simplified sounding system for finding NVIS channel availability to support government radio networks in Indonesia," *Emitter: International Journal of Engineering & Technology*, vol. 7, no. 1, pp. 326–342, 2019.

[8] C. Fallen, "Global ionosphere model validation using HAARP and WSPR," in *Proceedings of the AMS, 99th Annual Meeting*, Phoenix, AZ, USA, January 2019, https://ams.confex.com/ams/2019Annual/webprogram/Paper355283.html.

[9] W. D. Reeve, "Radio observations of the HAARP summer 2018 research campaign," Technical report, Haarp, Gakona, Alaska, 2018, https://reeve.com/Documents/Articles%20Papers/Reeve_HAARP_Obsv_Jul2018.pdf.

[10] H Wspr Research, "Campaign yields hundreds of reports on 40 and 80 meters," *QST*, vol. 102, no. 11, p. 83, 2018, http://www.arrl.org/news/haarp-s-wspr-research-campaign-yields-hundreds-of-reports-on-40-and-80-meters.

[11] F. Paramadina, T. Dutono, and T. B. Santoso, "Reverse engineering wspr on vhf frequency band," in *Proceedings of the 2020 International Electronics Symposium*, pp. 157–162, (IES), Surabaya, Indonesia, September 2020.

[12] M. Hartje and U. Walter, "WSPR radio beacon at neumayer station III for evaluation of southern hemisphere radio propagation expeditions to Antarctica: ANT-land 2019/20 neumayer station III, kohnen station," *Flight Operations and Field Campaigns*, pp. 43–50, 2020.

[13] M. A. Cervera, T. J. Harris, D. A. Holdsworth, D. J. Netherway, and C. Huang, "Ionosphere dynamics and applications," in *Ionospheric Effects on HF Radio Wave Propagation*, pp. 439–492, John Wiley &amp, Sons, Inc, Hoboken, NJ, USA, 2021.

[14] Z. Bruno and R. Ljiljana, *Cander, "Ionospheric Prediction and Forecasting"*, Springer Geophysics, Berlin, Germany, 2014.

[15] WSPRnet, "WSPR database," 2021, https://wsprnet.org/drupal/.

[16] C. Oler and T. Cohen, *"The 160-Meter Band: An Enigma Shrouded in Mystery"*, CQ Magazine, Hicksville, NY, USA, 1998.

[17] F. H. Hibberd, "Self-distortion of radio waves in the ionosphere, near the gyro frequency," *Journal of Atmospheric and Terrestrial Physics*, vol. 11, no. 2, pp. 102–110, May 1957.

[18] B. A. Witvliet, E. Van Maanen, G. J. Petersen et al., "The importance of circular polarization for diversity reception and MIMO in NVIS propagation," in *Proceedings of the European Conference on Antennas and Propagation*, pp. 3382–3386, The Hague, The Netherlands, April 2014.

[19] B. A. Witvliet and R. M. Alsina-Pagès, "Radio communication via near vertical incidence skywave propagation: an overview," *Telecommunication Systems*, vol. 66, no. 2, pp. 295–309, 2017.

[20] B. A. Witvliet, E. van Maanen, G. J. Petersen et al., "Near vertical incidence skywave propagation: elevation angles and optimum antenna height for horizontal dipole antennas," *IEEE Antennas and Propagation Magazine*, vol. 57, no. 1, pp. 129–146, 2015.

[21] F. Orga, M. Hervas, and R. M. Alsina-Pages, "Flexible low-cost SDR platform for HF communications: near vertical incidence skywave preliminary results," *IEEE Antennas and Propagation Magazine*, vol. 58, no. 6, pp. 49–56, 2016.

[22] M. Hervás, P. Bergadà, and R. M. Alsina-Pagès, "Ionospheric narrowband and wideband HF soundings for communications purposes: a review," *Sensors*, vol. 20, no. 9, p. 2486, 2020.

[23] J. Taylor and B. Walker, "WSPRing around the world," *QST, American Radio Relay League, Inc*, vol. 94, no. 11, pp. 30–32, 2010.

[24] H. Burkhardt and L. Barbosa, "Contributions to the application of the Viterbi algorithm," *IEEE Transactions on Information Theory*, vol. 31, no. 5, pp. 626–634, 1985.

[25] A. Talbot, "The WSPR coding process," 2021, http://www.g4jnt.com/wspr_coding_process.pdf.

[26] J. Taylor, "Wsjt (version 9.7)," 2020, https://physics.princeton.edu/pulsar/k1jt/.

[27] I. Technology Antenna, "Lwa II, long wire 3-30 MHz + choke balun," 2021, https://ita-antennas.com/en/long-wire/230-lwa-antenne-long-fil.html.

[28] M. Katsouris, "HF amateur bands preselector (160 m band included)," 2021, https://www.sv1afn.com/en/product-category-4/HF-Amateur-Bands-Preselector.html.

[29] H. W. Silver, *"Transmission lines" in the ARRL Handbook for Radio Communications 2021*, pp. 20.26–20.30, E. McCune, Newington, CT, USA, 98 edition, 2020.

[30] D. Miron, "Small Antenna design," *The Short Dipole*, pp. 23–31, Newnes/Elsevier, Amsterdam, Netherlands, 1 edition, 2006.

[31] R. D. Hunsucker and J. K. Hargreaves, "The high-latitude ionosphere and its effects on radio propagation," *Cambridge Atmospheric and Space Science Series*, Cambridge University Press, Cambridge, UK, 2003.

[32] K. Davies, *"Magnetoionic Theory" in Ionospheric Radio*, The Institution of Engineering and Technology, London, UK, 1990.

[33] J. M. Maso, J. Male, J. Porte, J. L. Pijoan, and D. Badia, "Ionospheric polarization techniques for robust NVIS remote sensing platforms," *Applied Sciences*, vol. 10, no. 11, p. 3730, 2020.